A 10-Year Survey of Tropical Cyclone Inner-Core Lightning Bursts and Their Relationship to Intensity Change

STEPHANIE N. STEVENSON AND KRISTEN L. CORBOSIERO

University at Albany, State University of New York, Albany, New York

MARK DEMARIA

NOAA/National Hurricane Center, Miami, Florida

JONATHAN L. VIGH

National Center for Atmospheric Research, Boulder, Colorado

(Manuscript received 10 July 2017, in final form 11 October 2017)

ABSTRACT

This study seeks to reconcile discrepancies between previous studies analyzing the relationship between lightning and tropical cyclone (TC) intensity change. Inner-core lightning bursts (ICLBs) were identified from 2005 to 2014 in North Atlantic (NA) and eastern North Pacific (ENP) TCs embedded in favorable environments (e.g., vertical wind shear $\leq 10\,\mathrm{m\,s^{-1}}$; sea surface temperatures $\geq 26.5°C$) using data from the World Wide Lightning Location Network (WWLLN) transformed onto a regular grid with 8-km grid spacing to replicate the expected nadir resolution of the Geostationary Lightning Mapper (GLM). Three hypothesized factors that could impact the 24-h intensity change after a burst were tested: 1) prior intensity change, 2) azimuthal burst location, and 3) radial burst location. Most ICLBs occurred in weak TCs (tropical depressions and tropical storms), and most TCs intensified (remained steady) 24 h after burst onset in the NA (ENP). TCs were more likely to intensify 24 h after an ICLB if they were steady or intensifying prior to burst onset. Azimuthally, 75% of the ICLBs initiated downshear, with 92% of downshear bursts occurring in TCs that remained steady or intensified. Of the ICLBs that initiated or rotated upshear, 2–3 times more were associated with TC intensification than weakening, consistent with recent studies finding more symmetric convection in intensifying TCs. The radial burst location relative to the radius of maximum wind (RMW) provided the most promising result: TCs with an ICLB inside (outside) the RMW were associated with intensification (weakening).

1. Introduction

Several recent studies have focused on the utility of lightning data to improve short-term (e.g., 24 h) tropical cyclone (TC) intensity forecasts; however, the relationship between lightning activity and TC intensity change is inconsistent among these studies. Earlier studies utilized lightning from the continent-based National Lightning Detection Network (NLDN; Molinari et al. 1994, 1999), the *Microlab-1* satellite's Optical Transient Detector (OTD; Cecil and Zipser 1999), Vaisala's Long-Range Lightning Detection Network (LLDN; Squires and Businger 2008), and the Tropical Rainfall Measuring Mission's (TRMM's) Lightning Imaging Sensor (LIS; Jiang and Ramirez 2013; Xu et al. 2017), while more recent studies have used global, ground-based lightning detection networks, such as the World Wide Lightning Location Network (WWLLN; Price et al. 2009; Pan et al. 2010, 2014; Abarca et al. 2011; DeMaria et al. 2012; Stevenson et al. 2014, 2016; Zhang et al. 2015; Zawislak et al. 2016; Rogers et al. 2016), to analyze the spatial and temporal characteristics of lightning in TCs.

The radial distribution of lightning in TCs has a distinct pattern with two maxima. Deep convection in both the inner core (~0–100 km) and outer rainbands (~200–300 km) exhibits the largest lightning frequency, with a distinct minimum in the stratiform-dominated inner rainband (~100–200 km), or moat, region (Molinari et al. 1999; Cecil et al. 2002; Abarca et al. 2011; Stevenson et al. 2016). The focus of this study is the inner-core maximum, which has been heavily researched in the recent literature

Corresponding author: Stephanie N. Stevenson, sstevenson@albany.edu

DOI: 10.1175/WAF-D-17-0096.1

with varying results concerning its relationship to TC intensity change.

In the northwest Pacific basin, large inner-core lightning flash rates were found in *intensifying* TCs (Zhang et al. 2015) prior to the maximum intensity (Pan et al. 2010, 2014). Several studies based in the eastern North Pacific and North Atlantic have found similar results (Molinari et al. 1994; Price et al. 2009; Abarca et al. 2011; Stevenson et al. 2014; Zawislak et al. 2016); however, the opposite relationship has also been noted in these basins, where a larger lightning flash density was evident in *weakening* TCs (DeMaria et al. 2012; Jiang and Ramirez 2013; Stevenson et al. 2016; Xu et al. 2017). Molinari et al. (1999) and Squires and Businger (2008) both noted cases where inner-core lightning outbreaks occurred either during rapid intensification or just prior to weakening.

The studies above utilized lightning networks that were either confined to regions near the coastline with a high detection efficiency (e.g., NLDN, LLDN), capable of capturing global lightning with a relatively low detection efficiency (e.g., WWLLN), or temporally confined to a 90-s snapshot of a region with a high detection efficiency (e.g., LIS, OTD). Additionally, these networks vary in the types of lightning they are able to detect. The NLDN primarily captures cloud-to-ground (CG) lightning, while the WWLLN is able to capture both CG and intracloud (IC) lightning, although the WWLLN detection efficiency of CG flashes is approximately twice that of IC flashes (Abarca et al. 2010). Although the LIS and OTD instruments were limited in their temporal sampling, they were able to detect *total* lightning (CG + IC) with high detection efficiency. Continuous coverage of *total lightning* in TCs will soon become available operationally with the Geostationary Lightning Mapper (GLM) instrument on board *Geostationary Operational Environmental Satellite-16* (*GOES-16*). The GLM will become the first instrument capable of providing the temporal evolution of lightning in TCs with high detection efficiency [estimated 70%–90%; Goodman et al. (2013)]; thus, any consistent relationships established between TC lightning activity and intensity change would be useful for predicting future TC intensities when the GLM data become available.

Potential reasons for the disparities in the sign of the intensity change following an inner-core lightning outbreak have been addressed by a few studies. First, Molinari et al. (1999) proposed that a weakening, steady, or slowly intensifying TC might be more likely to intensify after an inner-core lightning outbreak, whereas intensification may end or reverse if an inner-core lightning outbreak occurs in a TC that has been intensifying for some time.

Second, case studies by Fierro et al. (2011), Stevenson et al. (2014) and Rogers et al. (2016) showed that inner-core lightning outbreaks may be associated with intensification when they rotate upshear of the center. Many other recent satellite-based studies have shown that upshear convection often precedes intensification as a result of more symmetric heating around the TC center (Zagrodnik and Jiang 2014; Alvey et al. 2015; Fischer et al. 2017). The azimuthal distribution of convection and lightning in TCs are primarily controlled by the deep-layer environmental vertical wind shear (Corbosiero and Molinari 2003), with more active lightning downshear left (right) in the inner core (outer rainbands) (Corbosiero and Molinari 2002). The response of the TC vortex to the environmental vertical wind shear is thought to control this azimuthal distribution of lightning, such that a vortex tilted downshear will attempt to realign through an enhanced secondary circulation downshear (Reasor et al. 2004), resulting in deeper convection capable of producing lightning. However, Stevenson et al. (2014) showed a case where lightning peaked *upshear left*, consistent with the observed tilt of the TC vortex, prior to rapid intensification. This result led the authors of that study to hypothesize that the azimuthal location of an inner-core lightning burst may have implications on the future 24-h intensity change.

Third, Stevenson et al. (2014), Susca-Lopata et al. (2015), and Rogers et al. (2016) presented case studies where an inner-core lightning outbreak occurred radially inward of the radius of maximum wind (RMW) prior to intensification. Rogers et al. (2013) also found that deep convection, identified by updraft strength, was located radially inward (outward) of the RMW in intensifying (steady state) TCs. When convection is located inside the RMW, higher inertial stability radially confines the warming response, leading to a larger intensification of the vortex (Vigh and Schubert 2009). Dynamically, deep convection inside the RMW can force the secondary circulation, and thus the eyewall, to move radially inward, leading to TC intensification (Shapiro and Willoughby 1982; Smith and Montgomery 2016).

This study adopts an objective method of identifying inner-core lightning bursts (i.e., concentrated regions of deep convection) in North Atlantic and eastern North Pacific TCs from 2005 to 2014 using the WWLLN. The identified inner-core lightning bursts are analyzed with respect to three factors hypothesized to impact the 24-h intensity change: 1) the prior 24-h intensity change, 2) the azimuthal location of the burst, and 3) the radial location of the burst. The data and methods are described in section 2. Section 3a surveys the identified inner-core lightning bursts, and section 3b analyzes how the aforementioned factors impact the future 24-h

intensity change. A summary and conclusions are provided in section 4.

2. Data and methods

a. Inner-core lightning burst identification

An inner-core lightning burst (ICLB) is defined in this study to objectively identify *concentrated* regions of enhanced lightning flash density in the TC inner core. Lightning flash locations for all TCs in the eastern North Pacific (ENP) and North Atlantic (NA) from 2005 to 2014 were obtained from the WWLLN (operated by the University of Washington; http://wwlln.net). The WWLLN has provided continuous, global lightning coverage throughout the ENP and NA tropical cyclone seasons (May–November) since 2005 (Rodger et al. 2009), although detection efficiency has steadily increased as sensors have been added to the network. Similar to DeMaria et al. (2012), adjustment factors were applied to the WWLLN data in each basin using yearly lightning densities estimated from the LIS/OTD instruments' High Resolution Full Climatology dataset (Cecil 2001) to account for the growing network over the 10-yr study period (Table 1). Detection efficiencies are higher over ocean than over land for the WWLLN (Rudlosky and Shea 2013), ranging from 25% to 50% in the ENP and NA, making the WWLLN an ideal network with continuous observations for TC studies.

The locations of TCs were obtained from the National Hurricane Center (NHC) best-track dataset, which provides TC center locations in 6-h intervals. For this study, tracks are linearly interpolated to 1-h intervals to better capture the azimuthal and radial distribution of lightning. Despite the NHC best track's inability to capture erratic movement at shorter time intervals (Landsea and Franklin 2013), Stevenson et al. (2014) found similar lightning distributions when using a finer time resolution track from aircraft reconnaissance.

Lightning flash locations were transformed into lightning densities on an 8 km × 8 km spatial grid centered on the interpolated best-track center for each TC hour. The grid spacing was chosen to align with the expected nadir resolution of the *GOES-16* GLM (Goodman et al. 2013). Despite the WWLLN's location accuracy of approximately 10 km (Rodger et al. 2009; Rudlosky and Shea 2013), the most extreme lightning outbreaks in the inner core (i.e., ICLBs) were captured on the smaller spatial grid. For the purposes of this study, the traditional inner-core radial range [0–100 km; e.g., Corbosiero and Molinari (2002, 2003); DeMaria et al. (2012)] was kept for major hurricanes (i.e., Saffir–Simpson scale of category 3 or higher), while a larger radial range (0–150 km) was examined for weaker TCs.

TABLE 1. The adjustment factors applied to the WWLLN data for each year in the ENP and NA basins based on the yearly lightning densities from the LIS/OTD 0.5° High Resolution Full Climatology.

	ENP	NA
2005	94.7	20.8
2006	23.4	13.0
2007	24.5	13.3
2008	10.5	9.7
2009	5.5	5.7
2010	5.9	4.8
2011	4.7	4.3
2012	3.4	3.4
2013	3.0	3.5
2014	2.9	3.3

The variability of the inner-core radius is supported by RMW data from the Extended Flight Level Dataset for Tropical Cyclones (FLIGHT+; Vigh et al. 2016), which transforms all U.S. Air Force Reserve and National Oceanic and Atmospheric Administration (NOAA) radial legs that were at least 45 km in length and within 25 km of the TC center into a quality-controlled, storm-relative framework (Fig. 1). Weaker TCs [i.e., tropical depressions (TDs), tropical storms (TSs), and category 1 and 2 hurricanes (H1 and H2) on the Saffir–Simpson scale] have a nonnegligible RMW distribution that extends beyond 100 km.

ICLBs were identified by first finding the *maximum* hourly lightning flash density within the inner core that fell in the upper quartile of all TC hours that had at least one flash. For the ENP (NA), this required the maximum hourly flash density on the 8-km grid to be larger than 20.3 (17.9) × 10^{-3} flashes $km^{-2} min^{-1}$. Second, ICLBs were also required to have an *average* inner-core flash density (i.e., calculated over the entire 0–100 or 0–150 km from the TC center) that fell in the upper quartile of all TC hours with at least one flash. For the ENP (NA), this required the average hourly inner-core flash density to be larger than 8.9 (12.6) × 10^{-5} flashes $km^{-2} min^{-1}$. This second average flash density threshold in the ICLB identification ensures that the maximum flash density identified in the first step is not confined to one grid box, especially since large adjustment factors were applied to the WWLLN data early in the study period (see Table 1). Despite the large adjustment factors influencing these thresholds, particularly in the ENP, the results presented in this study were found to be robust even if the thresholds were lowered (not shown). Caution should be exercised, however, when comparing ENP and NA results, as the thresholds for ''extreme'' lightning bursts may not translate uniformly between basins.

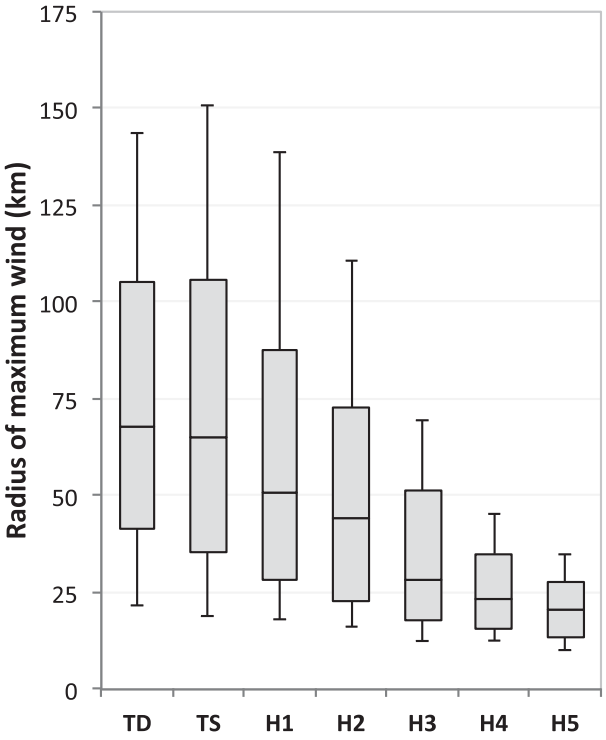

FIG. 1. Distributions of the RMW (km) as a function of TC intensity for all 2005–14 ENP and NA TCs in the FLIGHT+ dataset. Whiskers represent values at the 10th and 90th percentiles.

After TC hours with an ICLB were identified, the database was consolidated to remove duplicate ICLBs (i.e., bursts that lasted longer than 1 h), thus isolating the burst onset time. An ICLB was considered to be the same burst in consecutive hours if the distance traveled by the burst was less than the horizontal distance a parcel could travel given the maximum tangential wind speed from the NHC best track. Burst longevity will be briefly discussed in section 3, but the primary focus will be on the relationship between ICLB onset and future 24-h intensity change.

b. Environmental controls

Since the 24-h intensity change after the ICLB is the main focus of this study, ICLBs that occurred within 24 h of landfall were not included. Furthermore, environmental factors, such as sea surface temperature (SST) and vertical wind shear, are known to be strongly correlated with TC intensity change (Kaplan and DeMaria 2003). The Statistical Hurricane Intensity Prediction Scheme (SHIPS; DeMaria and Kaplan 1994) was used to obtain a weekly 1°-resolution Reynolds SST (Reynolds and Marsico 1993) and a deep-layer (850–200 hPa) vertical wind shear azimuthally averaged between the 200- and 800-km radii for each identified ICLB. Only TCs exhibiting SSTs $\geq$ 26.5°C and vertical wind shear $\leq$ 10 m s^{-1} at burst onset were included in an effort to further isolate the influence of an ICLB on TC intensity change. Gray (1968) stated that this SST threshold is a necessary, but insufficient, thermodynamic constraint for tropical cyclogenesis, and several studies have noted the negative impacts of strong vertical wind shear on TC intensity (DeMaria 1996; Frank and Ritchie 2001; Tang and Emanuel 2010).

3. Results and discussion

a. Survey of ICLBs

In the ENP (NA), 32% (51%) of all 17 814 h (14 594 h) observed in TCs from 2005 to 2014 exhibited at least one lightning flash in the inner core. A total of 1117 h (1573 h) met both the aforementioned maximum and average hourly lightning flash density criteria in the ENP (NA), resulting in 519 (705) uniquely identified ICLBs once hours beyond the burst onset time for long-duration bursts were excluded. Figure 2 highlights the locations within the basins where the ICLBs occurred, overlaid with climatological SSTs from the most active month in the respective basin. In both the ENP and NA, the bursts occurred more frequently in regions closer to landmasses and in regions of warm SSTs. Stevenson et al.'s (2016) "sweet spot" of 28°–30°C SSTs for lightning in TCs matches well with where the most extreme lightning flash rates were found. The sample size of ICLBs was reduced to 410 (443) in the ENP (NA) once the cases in unfavorable TC environments (i.e., SST $<$ 26.5°C and shear $>$ 10 m s^{-1}) were removed. For the remainder of this paper, only the ICLBs that were in favorable environments will be discussed.

The seasonal distribution of TC activity between 2005 and 2014 in the ENP (NA) was normally distributed with peak activity observed in August (September) (Figs. 3a,b, black lines). In the NA, the seasonal distribution of ICLBs (Fig. 3b, green line) was nearly identical to that of TC activity; however, in the ENP, a much more complex relationship was observed (Fig. 3a). The ENP experienced relative maxima in ICLB activity near the beginning of the season (May), during peak TC activity (August), and near the end of the season (October). Kucienska et al. (2012b) found a similar distribution in their study of lightning in the ENP, with maxima in May and August, and minima in June and September, consistent with periods of observed easterly and westerly winds, respectively (Romero-Centeno et al. 2007).

Many studies have attributed the seasonal patterns of rainfall and lightning to the nonlinear interactions with

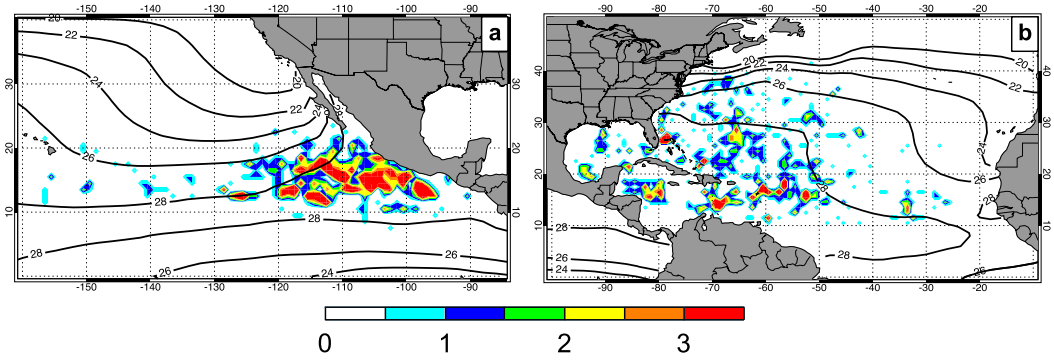

FIG. 2. The frequency of ICLBs (count; color fill) and the monthly mean SSTs (°C; black contours) in the (a) ENP and (b) NA. The August and September SSTs are shown for the ENP and NA, respectively, to align with the peak in seasonal activity. Climatological SST data from 1981 to 2010 were obtained from the NOAA Extended Reconstructed SST, version 3b.

SST fluctuations and changes in the dynamics and microphysics over the ENP. A maximum in deep convection over the ENP is reached when SSTs exceed 29°C around May (Waliser and Gautier 1993; Magaña et al. 1999), consistent with the first observed maxima in ICLBs. SSTs decrease afterward as convection limits the solar radiation (Magaña et al. 1999), and stronger easterly winds in July and August coincide with an increase in the strength of the Tehuantepec jet in southern Mexico (Romero-Centeno et al. 2007). Although precipitation is observed to decrease over both land and ocean during this time (sometimes referred to as the midsummer drought), the frequency of lightning increases as continental cloud condensation nuclei are transported several hundred kilometers offshore by the Tehuantepec jet, thus increasing the likelihood of the electrification of clouds over the oceans (Kucienska et al. 2012a). The spatial locations of the ICLBs, color coded by month, are shown in Figs. 3c and 3d. Many of the ICLBs near the Mexican coastline in the ENP

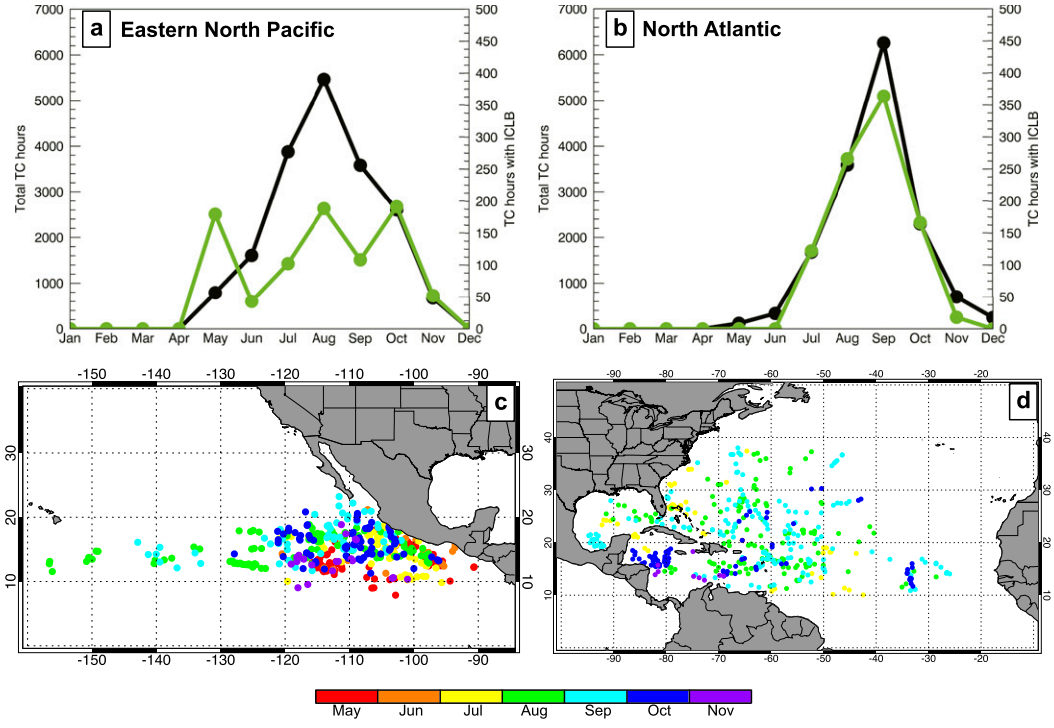

FIG. 3. The total number of TC hours from 2005 to 2014 (black) and the number of TCs hours with an ICLB (green) for the (a) ENP and (b) NA for each month. The spatial distribution of ICLBs for the (c) ENP and (d) NA is color coded by month.

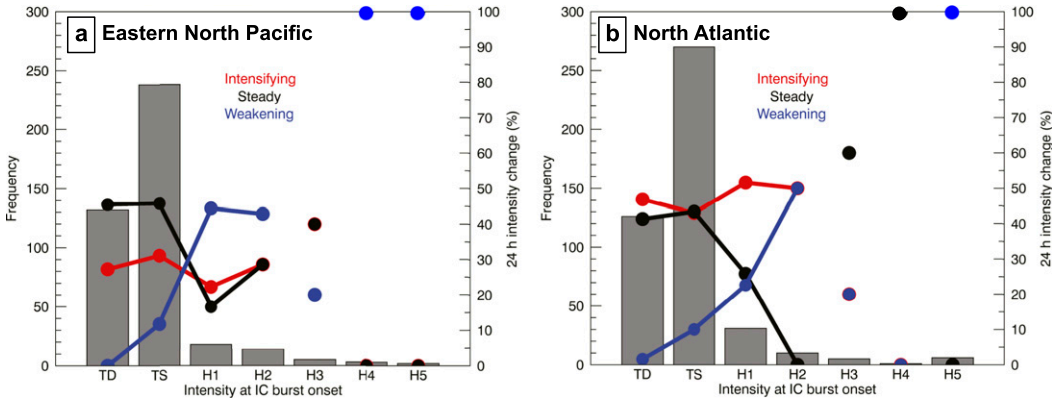

FIG. 4. Histograms of the frequency of ICLBs in favorable environments for varying TC intensities (gray bars) in the (a) ENP and (b) NA. Dots display the percentage of ICLBs in each TC intensity category that experienced TC intensification ($\Delta v_{24h} \geq 5\,m\,s^{-1}$; red), steadiness ($-5\,m\,s^{-1} < \Delta v_{24h} < 5\,m\,s^{-1}$; black), and weakening ($\Delta v_{24h} \leq -5\,m\,s^{-1}$; blue) 24 h after the burst onset, with lines drawn for TC intensity categories with at least 10 ICLBs.

occurred during May, July, August, and October. Previous studies have noted these months are characterized by a stronger jet in the Tehuantepec region and easterly zonal winds (i.e., a dynamic influence that perhaps provides a source of continental aerosols for oceanic convection to become electrified).

Figure 4 shows the distribution of ICLB occurrence as a function of TC intensity at the time of burst onset. Most ICLBs occurred in weak TCs (e.g., TD and TS) as expected, since previous studies have shown that weak TCs tend to produce larger lightning flash densities than strong TCs (Cecil and Zipser 1999; Abarca et al. 2011; DeMaria et al. 2012). It is worth noting that the climatological bias toward the occurrence of weak TCs in the database does not change this result, as a higher percentage of weak TCs had an observed ICLB when compared to strong TCs. Of the ICLBs in TCs that remained tropical (as defined by NHC) 24 h later, a large portion experienced either intensification ($\Delta v_{24h} \geq 5\,m\,s^{-1}$; 34% in ENP and 46% in NA) or remained steady ($-5\,m\,s^{-1} < \Delta v_{24h} < 5\,m\,s^{-1}$; 51% in ENP and 42% in NA), while a mere 11%–14% weakened ($\Delta v_{24h} \leq -5\,m\,s^{-1}$).

Figure 4 suggests that the likelihood of certain intensity changes varies based on the TC intensity at the time of the ICLB onset. TDs and TSs were more likely to intensify or remain steady, while strong TCs were more likely to weaken, which is a pattern that matches well with DeMaria and Kaplan's (1994) statistical analysis that found TCs farther from their theoretical maximum potential intensities were more often associated with intensification. These results indicate that most ICLBs are not associated with weakening and, in fact, a significantly larger fraction experience *intensification*. This contradicts DeMaria et al.'s (2012) findings in the same basins; however, their study analyzed average inner-core lightning densities in all TCs regardless of the shear or SSTs, while our study isolates concentrated regions of lightning in the inner core of TCs in favorable environments (i.e., low shear and warm SSTs). In fact, many of the cases with the largest inner-core lightning densities in DeMaria et al.'s (2012) study occurred in the presence of high shear and subsequently weakened (see their Table 2).

Burst longevity was comparable between the two basins, and no clear relationship between ICLB longevity and 24-h intensity change was found (not shown). Most (56%) of the identified ICLBs in a favorable environment only met both lightning density criteria for 1 h. Approximately 19% of the ICLBs lasted 2 h, and only 5% lasted 6 h or more. It is worth noting that lightning could have continued in these ICLBs for a longer duration; however, the methodology specifically isolates hours with extreme flash densities. For example, the ICLB in Hurricane Earl (2010), described in Stevenson et al. (2014), was captured for 4 h using the present methodology, despite evidence of the lightning continuing for a longer duration with lower flash densities (see their Fig. 7).

b. *Relationship to intensity change*

1) PRIOR INTENSITY CHANGE

The strongest signal that arose between the prior and future 24-h intensity changes was persistence (Fig. 5). In both basins, a large frequency of TCs that were intensifying prior to the ICLB onset continued to intensify afterward. The same holds true for the steady and weakening cases, with an exception being in the ENP with ICLBs in TCs that were weakening prior to burst

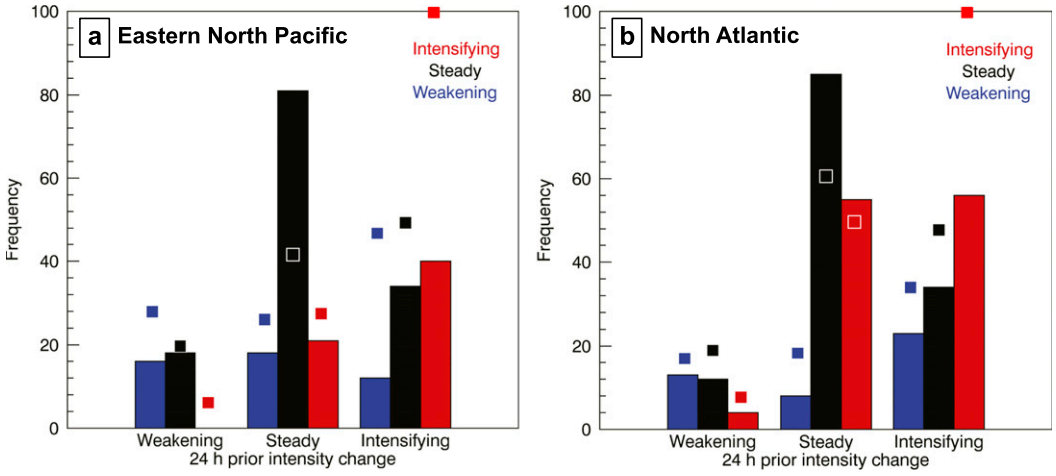

FIG. 5. The frequency of TCs in favorable environments that were weakening ($\Delta v_{24h} \leq -5\,m\,s^{-1}$; blue bars), steady ($-5\,m\,s^{-1} < \Delta v_{24h} < 5\,m\,s^{-1}$; black bars), and intensifying ($\Delta v_{24h} \geq 5\,m\,s^{-1}$; red bars) 24 h after an ICLB as a function of the 24-h prior intensity change in the (a) ENP and (b) NA. The normalized distributions of all 2005–14 TCs in a favorable environment are shown in squares for a climatological comparison.

onset, where a larger frequency fell in the "steady" intensity change category 24 h later. The climatological distributions shown in Fig. 5 suggest that the cases with an ICLB do not differ qualitatively from climatology; in fact, a Wilcoxon rank-sum test confirms that no significant differences exist between the ICLB distribution and the climatological distribution. At shorter time scales, DeMaria and Kaplan (1994) found a similar positive correlation between the prior and future 12-h intensity changes (i.e., persistence).

Portions of the prior intensity change hypothesis proposed by Molinari et al. (1999) are supported by the ICLB climatology in this study. TCs that were steady prior to an ICLB had a larger frequency of intensification rather than weakening 24 h after burst onset, a pattern more prevalent in the NA basin. However, contrary to Molinari et al.'s (1999) hypothesis, intensifying TCs that experienced an ICLB were not more likely to weaken afterward; in fact, the highest frequency of intensification following an ICLB occurred in TCs that were intensifying prior to the burst onset in both the ENP and NA. Approximately 56% (64%) of the TCs in the ENP (NA) with an ICLB that continued to intensify 24 h after a previous 24 h intensification period experienced an increase in the intensification rate, with the average intensification rate increasing by $6.7\,m\,s^{-1}$ ($7.8\,m\,s^{-1}$) (not shown). This finding aligns well with previous studies that have noted an increase in inner-core lightning activity during periods of TC intensification (Molinari et al. 1994, 1999; Squires and Businger 2008; Stevenson et al. 2014; Zawislak et al. 2016). While no definitive signal for future intensity change is apparent from the prior intensity change, the results do suggest that intensification following an ICLB is most likely to occur in TCs that were steady or intensifying in the 24 h prior, although a nonnegligible fraction of TCs with ICLBs also experienced weakening and steadiness.

2) AZIMUTHAL LOCATION

The azimuthal lightning distribution in TCs is predominately controlled by the direction of the deep-layer vertical wind shear (Corbosiero and Molinari 2003; Stevenson et al. 2016), such that 90% of lightning flashes occur downshear (Corbosiero and Molinari 2002); however, a few TCs have been observed with a majority of the lightning flashes *upshear* (Stevenson et al. 2014; Rogers et al. 2016). Approximately 75% of ENP and NA ICLBs identified in this study occurred downshear, slightly lower than the 90% of lightning flashes that Corbosiero and Molinari (2002) found to occur downshear. Of those ICLBs occurring downshear, approximately 55% occurred in the downshear-left (DL) quadrant, as expected from the TC vortex response in a sheared environment (Corbosiero and Molinari 2002, 2003). When a TC is embedded in vertical wind shear, the shear acts to tilt the TC vortex downshear. In response, the secondary circulation downshear becomes stronger in an effort to reduce the tilt and realign the vortex (Reasor et al. 2004). Jones (1995) discusses how the upper- and lower-level cyclonic potential vorticity anomalies of the tilted vortex interact with one another causing the tilt to precess cyclonically. The vortex tilt usually stabilizes in the DL quadrant where the vertical wind shear and vortex precession balance one another, leading to stronger convection DL in the inner core (Corbosiero and Molinari 2002).

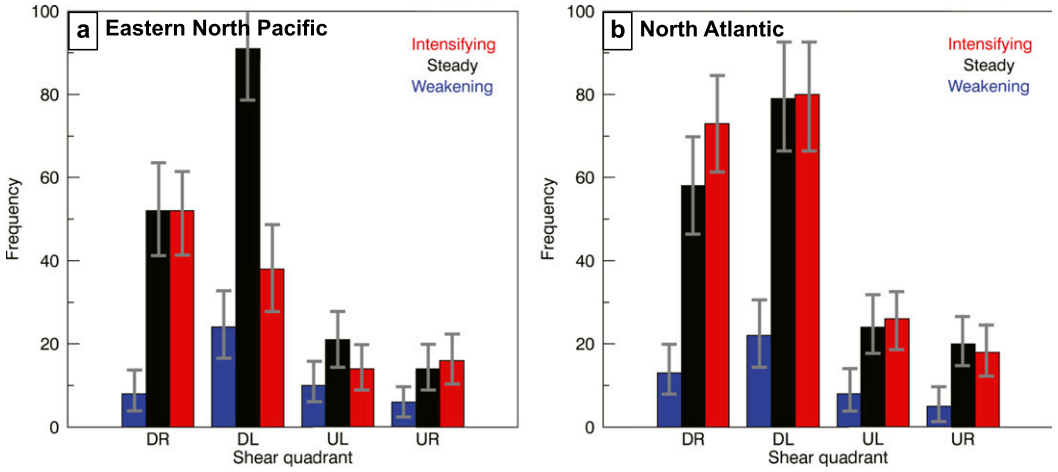

FIG. 6. The frequency of TCs in a favorable environment that were weakening ($\Delta v_{24h} \leq -5\ \mathrm{m\ s^{-1}}$; blue bars), steady ($-5\ \mathrm{m\ s^{-1}} < \Delta v_{24h} < 5\ \mathrm{m\ s^{-1}}$; black bars), and intensifying ($\Delta v_{24h} \geq 5\ \mathrm{m\ s^{-1}}$; red bars) 24 h after an ICLB as a function of the shear quadrant in the (a) ENP and (b) NA. The error bars indicate the range of statistical significance at the 95th percentile using a 10 000 iteration bootstrap resampling test with replacement. Quadrants are downshear right (DR), downshear left (DL), upshear left (UL), and upshear right (UR).

The 24-h intensity change following ICLB onset had a higher frequency of cases that intensified than weakened in all shear quadrants (Fig. 6). In the NA, nearly 4–5 times more TCs intensified, or remained steady, than weakened 24 h after the ICLB onset in all four shear quadrants (Fig. 6b); this relationship was found to be statistically significant using a 10 000-iteration bootstrap resampling test with replacement. This same relationship holds true for the downshear-right quadrant in the ENP (Fig. 6a); however, no statistically significant difference was found in the number of TCs that intensified, remained steady, or weakened with an ICLB observed in the upshear quadrants. Regardless, Fig. 6 suggests that the azimuthal location of burst *initiation* does not determine the intensity change 24 h later.

The motivation for analyzing the association between the azimuthal location of ICLBs and the 24-h intensity change came from Stevenson et al.'s (2014) finding of an ICLB in Hurricane Earl (2010) that *rotated* into the upshear-left quadrant near the beginning of rapid intensification. They showed the TC vortex tilted toward the upshear-left quadrant and hypothesized that the observed ICLB signaled that the vortex precessed upshear and contributed to intensification through vortex realignment from both the vertical wind shear and strong convection downtilt (Zhang and Tao 2013; Rios-Berrios et al. 2016). Figure 7 analyzes the rotation of ICLBs that persist for at least 4 h using the 6-h SHIPS deep-layer (850–200 hPa) vertical wind shear direction. The azimuthal path of ICLBs around the TC center in the NA was, on average, longer than that of ICLBs in the ENP (Table 2). Furthermore, a positive correlation was found between the 24-h intensity change and the mean pathlength of ICLBs in both basins, where TCs that intensified tended to have a longer azimuthal path than those that remained steady or weakened. This positive relationship remained consistent for median ICLB pathlengths in the NA. Ten of the 20 bursts in the NA that rotated into an upshear quadrant (Fig. 7b) occurred in TCs that intensified (red) compared to the three TCs that weakened (blue) and the seven TCs that remained steady (black), suggesting that rotation of an ICLB into the upshear quadrants may provide a signal that intensification is more likely over the next 24 h. This signal was not as evident in the ENP (Fig. 7a), where 6 of the 15 bursts that rotated in the upshear quadrants were associated with TC intensification, six TCs remained steady, and three TCs weakened.

Recently, studies have indicated that convection occurring upshear is favorable for intensification as it indicates that sufficient moisture exists at midlevels and a more symmetric diabatic heating signature can develop, despite the TC being located in a sheared environment (Guimond et al. 2010; Kieper and Jiang 2012; Zagrodnik and Jiang 2014; Alvey et al. 2015; Zawislak et al. 2016). Despite evidence in some cases that an ICLB beginning, or rotating, upshear was associated with intensification, the azimuthal location of the ICLB does not provide a definitive indication of future TC intensity change. It is worth noting that sufficient data do not exist to analyze the azimuthal ICLB location relative to the vortex *tilt*, which may be a more important contributing factor to the observed intensity change than the azimuthal

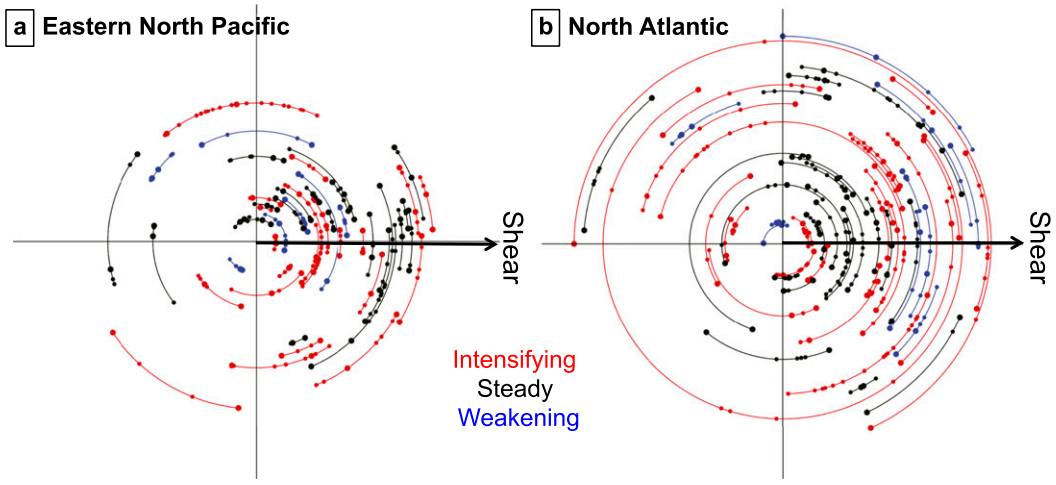

FIG. 7. The rotation of ICLBs relative to the shear vector that met the criteria for four or more hours for TCs in a favorable environment for the (a) ENP and (b) NA displayed as an ascending radial distance. The dots represent the shear-relative location for each hour of the ICLB, with larger dots indicative of the beginning and ending burst locations. Each long-lived burst is color coded by the 24-h intensity change following the ICLB onset: intensifying ($\Delta v_{24h} \geq 5\,m\,s^{-1}$; red), steady ($-5\,m\,s^{-1} < \Delta v_{24h} < 5\,m\,s^{-1}$; black), and weakening ($\Delta v_{24h} \leq -5\,m\,s^{-1}$; blue).

location relative to the shear, as was found in the case of Earl (2010) analyzed by Stevenson et al. (2014).

3) RADIAL LOCATION

The radial distribution of lightning has mostly been observed from the perspective of the distance from the TC center. As previously mentioned, lightning typically has a radial peak in the inner-core region (e.g., 0–100 km); however, the size of the inner core can vary with the size of the TC. The RMW is a distance measurement that, to some extent, accounts for TC size. A larger RMW is typically found in weaker TCs (see Fig. 1), and the RMW usually contracts as the TC intensifies (Shapiro and Willoughby 1982; Willoughby 1990); though, as Stern et al. (2015) showed, RMW contraction can sometimes cease in the middle of rapid intensification.

The location of the ICLBs relative to the RMW (r/RMW) and the subsequent 24-h intensity change are shown in Fig. 8. Measurements of the RMW are most accurately observed with aircraft reconnaissance; however, methods for determining the RMW from satellite-based methods are being developed (Knaff et al. 2015). For our study, the RMW was determined from flight-level winds in the FLIGHT+ dataset taken within 1 h of the ICLB onset time, limiting the sample size to 51 cases. It is worth noting that cases without a clearly defined RMW (e.g., those with a radially broad tangential wind maximum) and those without flight legs extending to at least 100 km were not included to isolate the relationship between ICLBs and TC intensity change in cases where the RMW was certain. The average 24-h intensity change of TCs with an ICLB inside the RMW (i.e., <1 RMW) was $5.3\,m\,s^{-1}$, with seven TCs intensifying and only one weakening after the ICLB onset. Immediately outside the RMW (i.e., 1–1.5 RMW), the average 24-h intensity change was $-2.6\,m\,s^{-1}$.

It should be noted that the FLIGHT+ dataset determines the RMW with respect to the Hurricane Research Division (HRD) Willoughby–Chelmow *flight-level* wind center (Willoughby and Chelmow 1982), while

TABLE 2. The count, median pathlength (km), and mean pathlength (km) of ICLBs displayed in Fig. 7 for each basin and intensity change category.

	24-h intensity change	ICLB count	Median pathlength (km)	Mean pathlength (km)
NA	Intensifying	26	119.7	144.6
	Steady	25	80.3	88.7
	Weakening	10	70.3	82.0
ENP	Intensifying	21	85.3	98.4
	Steady	21	63.1	87.8
	Weakening	7	86.6	79.8

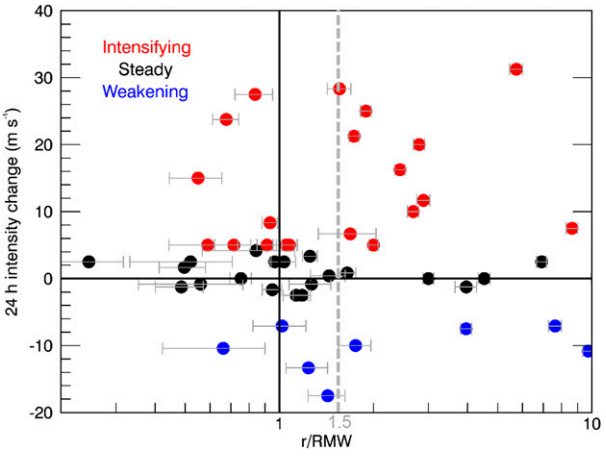

FIG. 8. The 24-h intensity change ($m\,s^{-1}$) of NA TCs with an ICLB relative to the RMW (r/RMW; logarithmic scale) with aircraft reconnaissance within 1 h of the observed ICLB. The errors bars indicate one standard deviation of 10 000 random errors (±0.2°) added to the NHC best-track position.

the NHC best-track database, which was used to locate the radial position of ICLBs in this study, represents a smoothed track of the geometric surface center of the TC. Despite this difference, a sensitivity analysis showed that the patterns of ICLBs with respect to the RMW remained largely the same regardless of which track position data were used to locate the ICLBs (not shown). Figure 8 contains error bars that indicate one standard deviation of 10 000 samples that added normally distributed random errors [±0.2°; consistent with the average position errors discussed in Landsea and Franklin (2013)] to the linearly interpolated NHC best-track positions. These error bounds demonstrate that the relationship between the RMW-relative ICLB location and subsequent intensity change is robust despite potential TC position errors that may exist in the best track.

Beyond 1.5 RMW, there was a larger preference for intensification in TCs with an ICLB, possibly related to rainband convection instead of inner-core convection. Although capturing rainband flashes is a side effect of using a fixed radius to define the inner core, the tendency for more TCs to intensify with bursts of lightning in the rainbands agrees with the findings of DeMaria et al. (2012) and Stevenson et al. (2016). We are investigating the relationship between outer rainband flashes and TC intensity change in ongoing research.

A spatial composite of the lightning densities for weakening, steady, and intensifying TCs relative to the RMW and vertical wind shear for the 51 cases in Fig. 8 is shown in Fig. 9. The weakening cases had the highest average lightning flash densities just outside the RMW (note that the lightning densities inside the RMW greater than 2.60×10^{-3} flashes $km^{-2}\,min^{-1}$ in Fig. 9a are associated with the outlier in Fig. 8 located at 0.66 RMW with a 24-h intensity change of $-10\,m\,s^{-1}$). The intensifying cases had two pronounced signals: 1) large lightning flash densities located at or inside the RMW, with a considerable lightning flash density located *upshear*, and 2) large lightning flash densities between 2 and 3 RMW, focused in the downshear-right quadrant where lightning typically peaks in the outer rainbands (Corbosiero and Molinari 2002). This latter result is consistent with the intensification noted above beyond 1.5 RMW and gives credence to the hypothesis that these are outer rainband flashes.

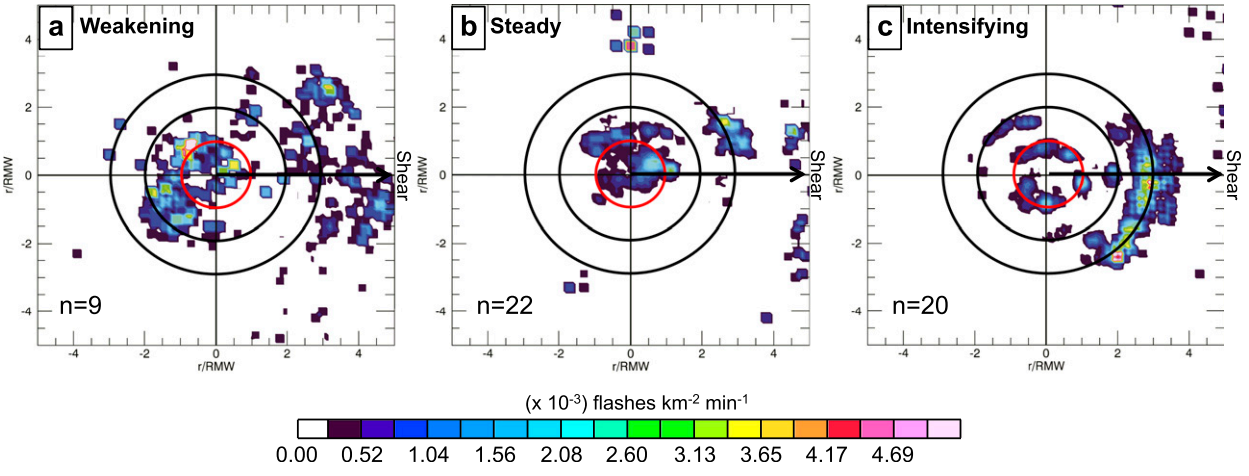

FIG. 9. The lightning density relative to the RMW for (a) weakening ($\Delta v_{24h} \le -5\,m\,s^{-1}$), (b) steady ($-5\,m\,s^{-1} < \Delta v_{24h} < 5\,m\,s^{-1}$), and (c) intensifying ($\Delta v_{24h} \ge 5\,m\,s^{-1}$) TCs for the 51 cases shown in Fig. 8. Radial rings are shown at the RMW (red), 2 × RMW, and 3 × RMW. The shear vector is pointing toward the right, and the number of ICLBs included in each composite is located in the bottom left of all panels.

Previous studies have advocated for the importance of convection relative to the RMW, both theoretically and observationally. Rogers et al. (2013) examined "convective bursts" based on the top 1% of vertical velocities from airborne Doppler observations and found a preference for bursts to be located radially inward of the RMW in intensifying TCs and radially outward of the RMW in steady-state TCs. Corbosiero et al. (2005) and Stevenson et al. (2014) highlighted convection inside the RMW of intensifying TC case studies using radar and lightning, respectively. The modeled response of the secondary circulation to a heat source (e.g., convection) at or inside the RMW leads to TC intensification (Shapiro and Willoughby 1982; Pendergrass and Willoughby 2009). Thermodynamically, diabatic heating from convection would be radially confined to the TC core and be more efficient for intensification since the region inside the RMW is characterized by a larger inertial stability (Vigh and Schubert 2009). Dynamically, the radial overturning circulation resulting from convection inside the RMW advects absolute angular momentum radially inward, contracting the RMW and intensifying the TC (Smith and Montgomery 2016). The *radial* location of the ICLBs had the most robust signal for reconciling the intensity change disparities found in previous TC lightning studies and holds the most promise for aiding in TC intensity forecasting.

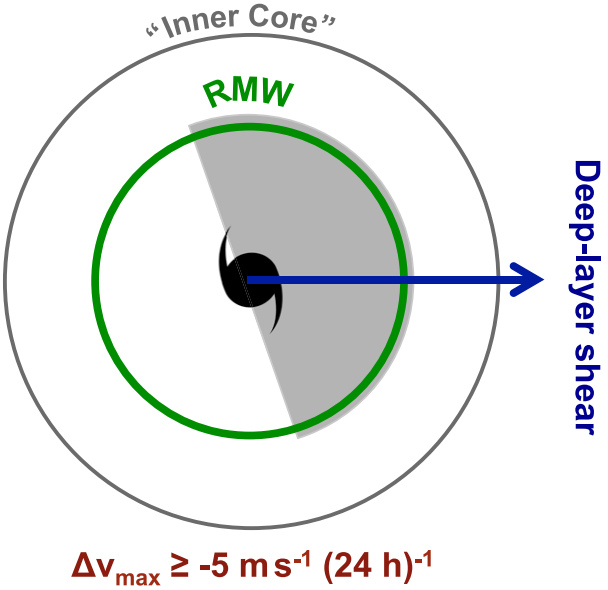

FIG. 10. A schematic summary highlighting the scenarios when an ICLB (gray shading) is most likely to be associated with TC intensification ($\Delta v_{24h} \geq 5\,m\,s^{-1}$) as it pertains to the three tested hypotheses: 1) the prior intensity change (maroon), 2) the location relative to the deep-layer vertical wind shear vector (dark blue), and 3) the location relative to the RMW (green).

4. Summary and conclusions

This study identifies ICLBs (i.e., concentrated regions of lightning activity in the TC inner core) on a spatial grid comparable to the expected *GOES-16* GLM resolution using lightning location data from the WWLLN between 2005 and 2014 in the ENP and NA basins. Most of the ICLBs identified in a favorable environment (i.e., low shear and warm SSTs) were associated with weak TCs (i.e., TDs and TSs) and intensified (remained steady) 24 h after burst onset in the NA (ENP). The identified ICLBs were used to test three hypothesized factors that could influence the 24-h intensity change:

- Prior intensity change—TCs that experienced an ICLB were most likely to intensify 24 h afterward if the TC was steady ($-5\,m\,s^{-1} < \Delta v_{24h} < 5\,m\,s^{-1}$) or intensifying ($\Delta v_{24h} \geq 5\,m\,s^{-1}$) prior to ICLB onset. The rate of intensification was found to increase in most TCs that were intensifying both 24 h before and after ICLBs.
- Azimuthal burst location—Most ICLBs *initiated* downshear, as expected, with most TCs intensifying or remaining steady 24 h afterward. Of the TCs with ICLBs that initiated upshear, a higher percentage intensified rather than weakened ($\Delta v_{24h} \leq -5\,m\,s^{-1}$); however, this relationship was found to be true in all shear quadrants in the NA, negating ICLBs initiated in the upshear quadrants as a distinguishing factor for the future 24-h intensity change. A majority of the long-lived (≥4 h) ICLBs that *rotated* into the upshear quadrants were in TCs that intensified, particularly in the NA basin, lending some credence to recent studies that more symmetric convection is beneficial to TC intensification.
- Radial burst location—The most robust result was that ICLBs that occurred at or inside the RMW were associated with TC intensification, whereas those just outside the RMW were associated with weakening. This compliments other observational and theoretical studies that have stressed the importance of a heating source (i.e., convection) radially inside the RMW for intensification.

Figure 10 shows a schematic summary of the scenario most likely to be associated with TC intensification in the presence of an ICLB (gray shading). This includes 1) a steady or intensifying TC 24 h prior to the ICLB onset, 2) an ICLB initiating in the downshear- or upshear-left quadrants, and 3) an ICLB located near or inside the RMW. The authors propose a graphic, such as the one shown in Fig. 11, that combines the lightning flash density, the flight-level RMW, and the deep-layer vertical wind shear direction to aid forecasters in determining if an

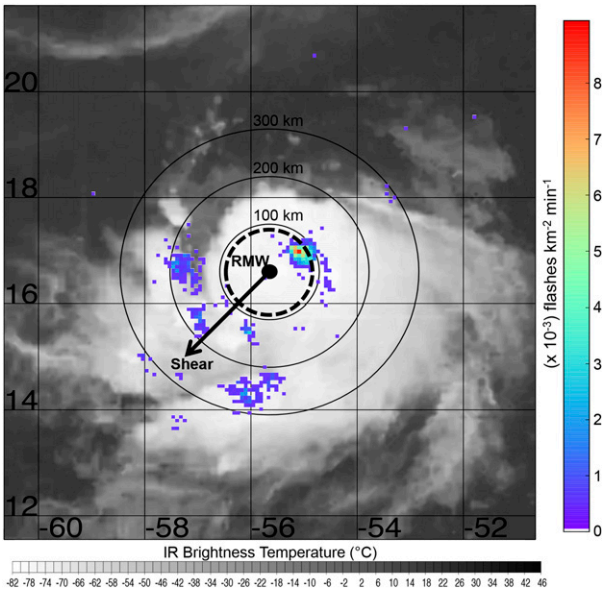

FIG. 11. A sample graphic that would aid forecasters in using lightning to forecast TC intensity change. This graphic combines infrared satellite brightness temperatures (°C; gray shading) for Hurricane Earl at 0300 UTC 29 Aug 2010, the WWLLN lightning density ($\times 10^{-3}$ flashes km^{-2} min^{-1}; color shading) from 0200 to 0300 UTC 29 Aug 2010 on an 8 km × 8 km grid, the NOAA WP-3D flight-level RMW (dashed black line), and the deep-layer (850–250 hPa) vertical wind shear (vector) to aid forecasters in determining the radial and azimuthal location of the ICLB.

ICLB fits the schematic in Fig. 10, indicating whether TC intensification is likely over the next 24 h.

Many recent studies utilizing regional and global lightning detection ground networks have found conflicting associations between lightning activity in the inner core and TC intensity change. This study isolates bursts within the inner core (rather than an average inner-core lightning flash density) and provides evidence that the *radial location relative to the RMW* is the most important factor in determining the sign of the intensity change 24 h after an ICLB. Thus, based on the results of prior studies with a robust sample size that found higher flash densities in weakening (intensifying) TCs in the North Atlantic (western North Pacific), one might hypothesize that deep convection is more likely to initiate in different RMW-relative radial regions across different TC basins and, as a result, the TCs undergo different average 24-h intensity changes. Nevertheless, the results from our study using data from the continuously sampling WWLLN, a network that detects IC flashes at a lower efficiency than CG flashes, suggest that the *GOES-16* GLM, a continuously sampling instrument with a high detection efficiency of both CG and IC flashes, will provide the most useful information to aid in TC intensity forecasts when lightning flash density is viewed in unison with the RMW (whether from flight reconnaissance or satellite-derived methods).

Acknowledgments. This work began as a project in a graduate-level Observations and Theory of Tropical Cyclones course at the University at Albany with the help of Casey Peirano. The project has been improved significantly over time, with financial support from UCAR COMET GOES-R Subaward Z15-20542. This work was supported by NASA Headquarters under the NASA Earth and Space Science Fellowship Program (Grant NNX15AN30H). We thank Michael Brennan, Christopher Landsea, Michael Fischer, and three anonymous reviewers for their comments and insightful suggestions. The authors wish to thank the World Wide Lightning Location Network (http://wwlln.net), a collaboration among over 50 universities and institutions, for providing the lightning location data used in this paper. The Extended Flight Level Dataset for Tropical Cyclones (FLIGHT+) was created by the Research Applications Laboratory at the National Center for Atmospheric Research (NCAR) from data provided by the NOAA Hurricane Research Division of the Atlantic Oceanographic and Meteorological Laboratory (AOML) and the U.S. Air Force Reserve. The creation of this dataset was funded through a grant from the Bermuda Institute of Ocean Sciences Risk Prediction Initiative (RPI2.0). NCAR is sponsored by the National Science Foundation. We thank Neal Dorst (AOML/HRD) for creating the wind center tracks and assembling the data and metadata that were vital for the creation of the FLIGHT+ dataset.

REFERENCES

Abarca, S. F., K. L. Corbosiero, and T. J. Galarneau Jr., 2010: An evaluation of the Worldwide Lightning Location Network (WWLLN) using the National Lightning Detection Network (NLDN) as ground truth. *J. Geophys. Res.*, **115**, D18206, https://doi.org/10.1029/2009JD013411.

——, ——, and D. Vollaro, 2011: The World Wide Lightning Location Network and convective activity in tropical cyclones. *Mon. Wea. Rev.*, **139**, 175–191, https://doi.org/10.1175/2010MWR3383.1.

Alvey, G. R., III, J. Zawislak, and E. Zipser, 2015: Precipitation properties observed during tropical cyclone intensity change. *Mon. Wea. Rev.*, **143**, 4476–4492, https://doi.org/10.1175/MWR-D-15-0065.1.

Cecil, D. J., 2001: LIS/OTD 0.5 degree High Resolution Full Climatology (HRFC). NASA Global Hydrology Center DAAC, Hunstville, AL, accessed 13 July 2015, doi:10.5067/LIS/LIS-OTD/DATA302.

——, and E. J. Zipser, 1999: Relationship between tropical cyclone intensity and satellite-based indicators of inner core convection: 85-GHz ice-scattering signature and lightning. *Mon. Wea. Rev.*, **127**, 103–123, https://doi.org/10.1175/1520-0493(1999)127<0103:RBTCIA>2.0.CO;2.

——, ——, and S. W. Nesbitt, 2002: Reflectivity, ice scattering, and lightning characteristics of hurricane eyewalls and rainbands.

Part I: Quantitative description. *Mon. Wea. Rev.*, **130**, 769–784, https://doi.org/10.1175/1520-0493(2002)130<0769:RISALC>2.0.CO;2.

Corbosiero, K. L., and J. Molinari, 2002: The effects of vertical wind shear on the distribution of convection in tropical cyclones. *Mon. Wea. Rev.*, **130**, 2110–2123, https://doi.org/10.1175/1520-0493(2002)130<2110:TEOVWS>2.0.CO;2.

——, and ——, 2003: The relationship between storm motion, vertical wind shear, and convective asymmetries in tropical cyclones. *J. Atmos. Sci.*, **60**, 366–376, https://doi.org/10.1175/1520-0469(2003)060<0366:TRBSMV>2.0.CO;2.

——, ——, and M. L. Black, 2005: The structure and evolution of Hurricane Elena (1985). Part I: Symmetric intensification. *Mon. Wea. Rev.*, **133**, 2905–2921, https://doi.org/10.1175/MWR3010.1.

DeMaria, M., 1996: The effect of vertical wind shear on tropical cyclone intensity change. *J. Atmos. Sci.*, **53**, 2076–2087, https://doi.org/10.1175/1520-0469(1996)053<2076:TEOVSO>2.0.CO;2.

——, and J. Kaplan, 1994: A statistical hurricane intensity prediction scheme (SHIPS) for the Atlantic basin. *Wea. Forecasting*, **9**, 209–220, https://doi.org/10.1175/1520-0434(1994)009<0209:ASHIPS>2.0.CO;2.

——, R. T. DeMaria, J. A. Knaff, and D. Molenar, 2012: Tropical cyclone lightning and rapid intensity change. *Mon. Wea. Rev.*, **140**, 1828–1842, https://doi.org/10.1175/MWR-D-11-00236.1.

Fierro, A. O., X. Shao, T. Hamlin, J. M. Reisner, and J. Harlin, 2011: Evolution of eyewall convective events as indicated by intracloud and cloud-to-ground lightning activity during the rapid intensification of Hurricanes Rita and Katrina. *Mon. Wea. Rev.*, **139**, 1492–1504, https://doi.org/10.1175/2010MWR3532.1.

Fischer, M. S., B. H. Tang, and K. L. Corbosiero, 2017: Assessing the influence of upper-tropospheric troughs on tropical cyclone intensification rates after genesis. *Mon. Wea. Rev.*, **145**, 1295–1313, https://doi.org/10.1175/MWR-D-16-0275.1.

Frank, W. M., and E. A. Ritchie, 2001: Effects of vertical wind shear on the intensity and structure of numerically simulated hurricanes. *Mon. Wea. Rev.*, **129**, 2249–2269, https://doi.org/10.1175/1520-0493(2001)129<2249:EOVWSO>2.0.CO;2.

Goodman, S. J., and Coauthors, 2013: The GOES-R Geostationary Lightning Mapper (GLM). *Atmos. Res.*, **125–126**, 34–49, https://doi.org/10.1016/j.atmosres.2013.01.006.

Gray, W. M., 1968: Global view of the origin of tropical disturbances and storms. *Mon. Wea. Rev.*, **96**, 669–700, https://doi.org/10.1175/1520-0493(1968)096<0669:GVOTOO>2.0.CO;2.

Guimond, S. R., G. M. Heymsfield, and F. J. Turk, 2010: Multiscale observations of Hurricane Dennis (2005): The effects of hot towers on rapid intensification. *J. Atmos. Sci.*, **67**, 633–654, https://doi.org/10.1175/2009JAS3119.1.

Jiang, H., and E. M. Ramirez, 2013: Necessary conditions for tropical cyclone rapid intensification as derived from 11 years of TRMM data. *J. Climate*, **26**, 6459–6470, https://doi.org/10.1175/JCLI-D-12-00432.1.

Jones, S. C., 1995: The evolution of vortices in vertical shear. I: Initially barotropic vortices. *Quart. J. Roy. Meteor. Soc.*, **121**, 821–851, https://doi.org/10.1002/qj.49712152406.

Kaplan, J., and M. DeMaria, 2003: Large-scale characteristics of rapidly intensifying tropical cyclones in the North Atlantic basin. *Wea. Forecasting*, **18**, 1093–1108, https://doi.org/10.1175/1520-0434(2003)018<1093:LCORIT>2.0.CO;2.

Kieper, M., and H. Jiang, 2012: Predicting tropical cyclone rapid intensification using the 37 GHz ring pattern identified from passive microwave measurements. *Geophys. Res. Lett.*, **39**, L13804, https://doi.org/10.1029/2012GL052115.

Knaff, J. A., S. P. Longmore, R. T. DeMaria, and D. A. Molenar, 2015: Improved tropical-cyclone flight-level wind estimates using routine infrared satellite reconnaissance. *J. Appl. Meteor. Climatol.*, **54**, 463–478, https://doi.org/10.1175/JAMC-D-14-0112.1.

Kucienska, B., G. B. Raga, and R. Romero-Centeno, 2012a: High lightning activity in maritime clouds near Mexico. *Atmos. Chem. Phys.*, **12**, 8055–8072, https://doi.org/10.5194/acp-12-8055-2012.

——, ——, and V. M. Torres-Puente, 2012b: Climatology of precipitation and lightning over the Pacific coast of southern Mexico retrieved from Tropical Rainfall Measuring Mission satellite products and World Wide Lightning Location Network data. *Int. J. Remote Sens.*, **33**, 2831–2850, https://doi.org/10.1080/01431161.2011.621905.

Landsea, C. W., and J. L. Franklin, 2013: Atlantic hurricane database uncertainty and presentation of a new database format. *Mon. Wea. Rev.*, **141**, 3576–3592, https://doi.org/10.1175/MWR-D-12-00254.1.

Magaña, V., J. A. Amador, and S. Medina, 1999: The midsummer drought over Mexico and Central America. *J. Climate*, **12**, 1577–1588, https://doi.org/10.1175/1520-0442(1999)012<1577:TMDOMA>2.0.CO;2.

Molinari, J., P. Moore, V. Idone, R. Henderson, and A. Saljoughy, 1994: Cloud-to-ground lightning in Hurricane Andrew. *J. Geophys. Res.*, **99**, 16 665–16 676, https://doi.org/10.1029/94JD00722.

——, ——, and ——, 1999: Convective structure of hurricanes as revealed by lightning locations. *Mon. Wea. Rev.*, **127**, 520–534, https://doi.org/10.1175/1520-0493(1999)127<0520:CSOHAR>2.0.CO;2.

Pan, L., X. Qie, D. Liu, D. Wang, and J. Yang, 2010: The lightning activities in super typhoons over the northwest Pacific. *Sci. China Earth Sci.*, **53**, 1241–1248, https://doi.org/10.1007/s11430-010-3034-z.

——, ——, and D. Wang, 2014: Lightning activity and its relation to the intensity of typhoons over the northwest Pacific Ocean. *Adv. Atmos. Sci.*, **31**, 581–592, https://doi.org/10.1007/s00376-013-3115-y.

Pendergrass, A. G., and H. E. Willoughby, 2009: Diabatically induced secondary flows in tropical cyclones. Part I: Quasi-steady forcing. *Mon. Wea. Rev.*, **137**, 805–821, https://doi.org/10.1175/2008MWR2657.1.

Price, C., M. Asfur, and Y. Yair, 2009: Maximum hurricane intensity preceded by increase in lightning frequency. *Nat. Geosci.*, **2**, 329–332, https://doi.org/10.1038/ngeo477.

Reasor, P. D., M. T. Montgomery, and L. D. Grasso, 2004: A new look at the problem of tropical cyclones in vertical shear flow: Vortex resiliency. *J. Atmos. Sci.*, **61**, 3–22, https://doi.org/10.1175/1520-0469(2004)061<0003:ANLATP>2.0.CO;2.

Reynolds, R. W., and D. C. Marsico, 1993: An improved real-time global sea surface temperature analysis. *J. Climate*, **6**, 114–119, https://doi.org/10.1175/1520-0442(1993)006<0114:AIRTGS>2.0.CO;2.

Rios-Berrios, R., R. D. Torn, and C. A. Davis, 2016: An ensemble approach to investigate tropical cyclone intensification in sheared environments. Part II: Ophelia (2011). *J. Atmos. Sci.*, **73**, 1555–1575, https://doi.org/10.1175/JAS-D-15-0245.1.

Rodger, C. J., J. B. Brundell, R. H. Holzworth, and E. H. Lay, 2009: Growing detection efficiency of the World Wide Lightning Location Network. *AIP Conf. Proc.*, **1118**, https://doi.org/10.1063/1.3137706.

Rogers, R., P. Reasor, and S. Lorsolo, 2013: Airborne Doppler observations of the inner-core structural differences between intensifying and steady-state tropical cyclones. *Mon. Wea. Rev.*, **141**, 2970–2991, https://doi.org/10.1175/MWR-D-12-00357.1.

——, J. A. Zhang, J. Zawislak, H. Jiang, G. R. Alvey III, E. J. Zipser, and S. N. Stevenson, 2016: Observations of the structure and evolution of Hurricane Eduoard (2014) during intensity change. Part II: Kinematic structure and the distribution of deep convection. *Mon. Wea. Rev.*, **144**, 3355–3376, https://doi.org/10.1175/MWR-D-16-0017.1.

Romero-Centeno, R., J. Zavala-Hidalgo, and G. B. Raga, 2007: Midsummer gap winds and low-level circulation over the eastern tropical Pacific. *J. Climate*, **20**, 3768–3784, https://doi.org/10.1175/JCLI4220.1.

Rudlosky, S. D., and D. T. Shea, 2013: Evaluation WWLLN performance relative to TRMM/LIS. *Geophys. Res. Lett.*, **40**, 2344–2348, https://doi.org/10.1002/grl.50428.

Shapiro, L. J., and H. E. Willoughby, 1982: The response of balanced hurricanes to local sources of heat and momentum. *J. Atmos. Sci.*, **39**, 378–394, https://doi.org/10.1175/1520-0469(1982)039<0378:TROBHT>2.0.CO;2.

Smith, R. K., and M. T. Montgomery, 2016: The efficiency of diabatic heating and tropical cyclone intensification. *Quart. J. Roy. Meteor. Soc.*, **142**, 2081–2086, https://doi.org/10.1002/qj.2804.

Squires, K., and S. Businger, 2008: The morphology of eyewall lightning outbreaks in two category 5 hurricanes. *Mon. Wea. Rev.*, **136**, 1706–1726, https://doi.org/10.1175/2007MWR2150.1.

Stern, D. P., J. L. Vigh, D. S. Nolan, and F. Zhang, 2015: Revisiting the relationship between eyewall contraction and intensification. *J. Atmos. Sci.*, **72**, 1283–1306, https://doi.org/10.1175/JAS-D-14-0261.1.

Stevenson, S. N., K. L. Corbosiero, and J. Molinari, 2014: The convective evolution and rapid intensification of Hurricane Earl (2010). *Mon. Wea. Rev.*, **142**, 4364–4380, https://doi.org/10.1175/MWR-D-14-00078.1.

——, ——, and S. F. Abarca, 2016: Lightning in eastern North Pacific tropical cyclones: A comparison to the North Atlantic. *Mon. Wea. Rev.*, **144**, 225–239, https://doi.org/10.1175/MWR-D-15-0276.1.

Susca-Lopata, G., J. Zawislak, and E. J. Zipser, 2015: The role of observed environmental conditions and precipitation evolution in the rapid intensification of Hurricane Earl (2010). *Mon. Wea. Rev.*, **143**, 2207–2223, https://doi.org/10.1175/MWR-D-14-00283.1.

Tang, B., and K. Emanuel, 2010: Midlevel ventilation's constraint on tropical cyclone intensity. *J. Atmos. Sci.*, **67**, 1817–1830, https://doi.org/10.1175/2010JAS3318.1.

Vigh, J. L., and W. H. Schubert, 2009: Rapid development of the tropical cyclone warm core. *J. Atmos. Sci.*, **66**, 3335–3350, https://doi.org/10.1175/2009JAS3092.1.

——, and Coauthors, 2016: FLIGHT+: The extended flight level dataset for tropical cyclones (version 1.1). Tropical Cyclone Data Project, Research Applications Laboratory, National Center for Atmospheric Research, Boulder, CO, accessed 27 September 2016, http://dx.doi.org/10.5065/D6WS8R93.

Waliser, D. E., and C. Gautier, 1993: A satellite-derived climatology of the ITCZ. *J. Climate*, **6**, 2162–2174, https://doi.org/10.1175/1520-0442(1993)006<2162:ASDCOT>2.0.CO;2.

Willoughby, H. E., 1990: Temporal changes of the primary circulation in tropical cyclones. *J. Atmos. Sci.*, **47**, 242–264, https://doi.org/10.1175/1520-0469(1990)047<0242:TCOTPC>2.0.CO;2.

——, and M. B. Chelmow, 1982: Objective determination of hurricane tracks from aircraft observations. *Mon. Wea. Rev.*, **110**, 1298–1305, https://doi.org/10.1175/1520-0493(1982)110<1298:ODOHTF>2.0.CO;2.

Xu, W., S. A. Rutledge, and W. Zhang, 2017: Relationships between total lightning, deep convection, and tropical cyclone intensity change. *J. Geophys. Res. Atmos.*, **122**, 7047–7063, https://doi.org/10.1002/2017JD027072.

Zagrodnik, J. P., and H. Jiang, 2014: Rainfall, convection, and latent heating distributions in rapidly intensifying tropical cyclones. *J. Atmos. Sci.*, **71**, 2789–2809, https://doi.org/10.1175/JAS-D-13-0314.1.

Zawislak, J., H. Jiang, G. R. Alvey III, E. J. Zipser, R. F. Rogers, J. A. Zhang, and S. N. Stevenson, 2016: Observations of the structure and evolution of Hurricane Eduoard (2014) during intensity change. Part I: Relationship between the thermodynamic structure and precipitation. *Mon. Wea. Rev.*, **144**, 3333–3354, https://doi.org/10.1175/MWR-D-16-0018.1.

Zhang, F., and D. Tao, 2013: Effects of vertical wind shear on the predictability of tropical cyclones. *J. Atmos. Sci.*, **70**, 975–983, https://doi.org/10.1175/JAS-D-12-0133.1.

Zhang, W., Y. Zhang, D. Zheng, F. Wang, and L. Xu, 2015: Relationship between lightning activity and tropical cyclone intensity over the northwest Pacific. *J. Geophys. Res. Atmos.*, **120**, 4072–4089, https://doi.org/10.1002/2014JD022334.